第 17 卷第 2 期 2019 年 4 月
1672-6553/2019/17(2)/136-7

动力学与控制学报
JOURNAL OF DYNAMICS AND CONTROL

Vol.17 No.2
Apr. 2019

双叶片整体叶盘的非线性振动分析*

揭晓博† 张伟

(北京工业大学 机电学院, 北京 100022)

摘要 论文研究了双叶片整体叶盘的非线性振动问题,将双旋转叶片简化为弹簧-旋转曲壳系统,考虑叶片的预安装角和预扭转角的影响,利用 Hamilton 原理建立了整体叶盘的非线性偏微分运动方程.综合运用 Galerkin 方法和数值方法,对模型进行了非线性动力学分析,模拟不同转速和激励作用下的叶片运动,得到波形图、相位图和功率谱密度,讨论了转速和外载荷对系统的非线性动力学特性的影响.

关键词 整体叶盘, 非线性动力学, 圆锥壳, Hamilton 原理, Galerkin 方法

DOI: 10.6052/1672-6553-2018-053

引言

压气机是航空发动机的重要组成部分之一.压气机叶片受到很大的离心惯性力和气动力作用,此外还有气流微振引起的振动及振动应力,并存在砂砾和叶片掉块等冲击损伤的危险.压气机叶片是直接影响发动机性能、可靠性和寿命的关键零件.因此,对叶片振动问题的研究具有非常重要的工程意义.本文主要研究航空发动机压气机双旋转叶片耦合振动的非线性动力学问题.

Rao[1] 等将涡轮叶片考虑为有固定转速的悬臂梁,用 Galerkin 法分别研究了带有弯扭耦合和扭转楔形梁的固有频率.Christensen[2] 等建立轴扭转和叶片弯曲变形耦合的动力学模型,基于弹性小变形理论,采用 Lagrange 法和有限元法推导旋转叶片系统的动力学方程,解释了叶片的振动现象.晏水平[3] 等将叶片简化为欧拉伯努利梁模型,根据梁在恒定轴向力用下的横向振动方程,计算在不同分布轴向力作用下悬臂梁的固有频率.Chen 和 Yao[4] 等考虑了离心力、气动力和几何非线性等因素,根据 Hamilton 原理和几何大变形理论,研究了存在预扭转角和预安装角的高速旋转叶片非线性动力学响应.Xiao 和 Chen[5] 用 Hamilton 原理建立了连接在刚体上的矩形薄板的非线性动力学模型,从理论上证明了刚柔耦合现象对非线性运动的影响.Hu[6] 等将叶片简化成弯曲的扭转圆柱薄板模型,利用虚功原理、Rayleigh-Ritz 方法分析了各参数对振动的影响.吴根勇[7] 等根据经典层合板理论,运用 Lagrange 原理和有限元法研究铺设层、铺设角和轮毂半径等因素对旋转复合材料板非线性振动响应造成的影响.Farhadi 和 Hashemi[8] 等将叶片简化成矩形旋转板模型,利用一阶剪切理论和冯卡门大变形理论,对叶片的颤振等动力学行为进行了研究.邓军和陈国平[9] 运用 Kirchhoff 假设,建立了匀速旋转薄板在分布动载荷下的动力学控制方程,并通过数值模拟得到了叶片振动响应.王晓峰,徐可君和秦海勤[10] 利用有限元分析技术,研究了不同参数对叶片模态的影响.

本文主要研究双旋转叶片整体叶盘耦合振动的非线性动力学问题.考虑叶片的预安装角和预扭转角的影响,利用 Hamilton 原理建立了横向外力作用下叶片的非线性偏微分运动方程.综合运用 Galerkin 方法和数值方法,研究了叶片的非线性动力学行为.

1 叶片非线性动力学模型

考虑第 $s(s=1,2)$ 个安装在半径为 r_0 的刚性轮毂上的旋转圆锥壳,该壳绕转轴旋转,其中转速为 $\Omega(t)=\Omega_c+\Omega_v\cos\omega_r t$, 如图 1 所示.坐标系

2018-03-13 收到第 1 稿,2018-05-21 收到修改稿.
* 国家自然科学基金资助项目(11290152,11427801)
† 通讯作者 E-mail:iron_man1945@163.com

$(x_{(s)},\theta_{(s)},z_{(s)})$位于圆锥壳的中面,任意点在 $x_{(s)}$,$\theta_{(s)}$和 $z_{(s)}$方向上的位移$(u_{(s)},v_{(s)},w_{(s)})$,$\varphi_{x\ (s)}$和 $\varphi_{\theta(s)}$分别表示中面绕 $\theta_{(s)}$和 $x_{(s)}$轴的转角.圆锥壳的几何参数分别为大端半径 $r_{\mathrm{root}(s)}$,预安装角 $\beta_{(s)}$,沿母线任意点半径为 $R_{(s)}=r_{\mathrm{root}(s)}-x_{(s)}\tan\psi_{(s)}$,预扭转角 $\Phi_{(s)}$,锥顶角为 $\alpha_{(s)}$,母线长 $L_{(s)}$,厚度 $h_{(s)}$.安装在叶片(x_p,y_p)处的忽略质量弹簧 $K_{(s)}$连接第 s 个叶片和第 s+1 个叶片,圆锥壳上表面均匀分布横向外力 $F_{(s)}=F_{0(s)}+F_{1(s)}\cos\omega_r t$,其中力 $F_{(s)}$由一个常量和简谐量构成.

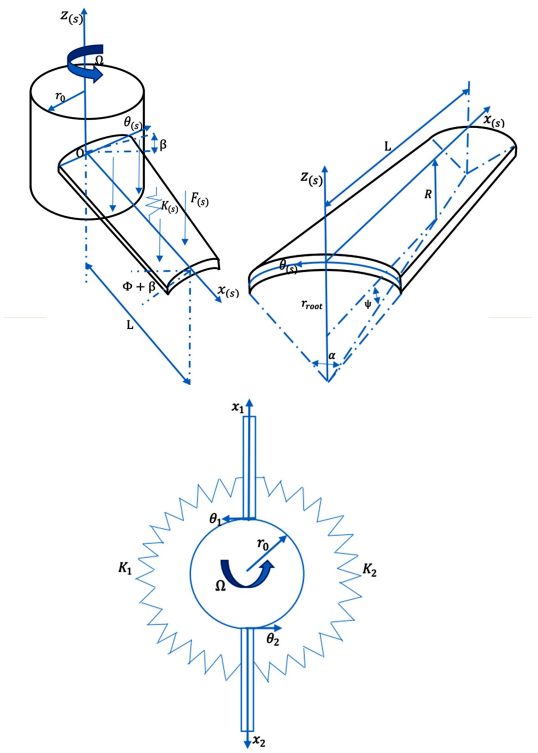

图 1　双叶片整体叶盘模型

Fig.1　Model of the bladed disk with two blades

根据一阶剪切变形理论,圆锥壳的位移场可以写为

$$u_{(s)}(x_{(s)},\theta_{(s)},z_{(s)},t)=u_{0(s)}(x_{(s)},\theta_{(s)},t)+z_{(s)}\varphi_{x(s)}(x_{(s)},\theta_{(s)},t)\quad(1a)$$

$$v_{(s)}(x_{(s)},\theta_{(s)},z_{(s)},t)=v_{0(s)}(x_{(s)},\theta_{(s)},t)+z_{(s)}\varphi_{\theta(s)}(x_{(s)},\theta_{(s)},t)\quad(1b)$$

$$w_{(s)}(x_{(s)},\theta_{(s)},z_{(s)},t)=w_{0(s)}(x_{(s)},\theta_{(s)},t)\quad(1c)$$

其中,$(s=1,2)$,$(u_{0(s)},v_{0(s)},w_{0(s)})$为圆锥壳中面任意一点的位移,$\varphi_{x(s)}$和 $\varphi_{\theta(s)}$分别表示中面绕 $\theta_{(s)}$和 $x_{(s)}$轴的转角.

非线性位移-应变关系可写为

$$\begin{bmatrix}\varepsilon_{x(s)}\\ \varepsilon_{\theta(s)}\\ \gamma_{x\theta(s)}\end{bmatrix}=\begin{bmatrix}\varepsilon^{(0)}_{x(s)}\\ \varepsilon^{(0)}_{\theta(s)}\\ \gamma^{(0)}_{x\theta(s)}\end{bmatrix}+z_{(s)}\begin{bmatrix}\varepsilon^{(1)}_{x(s)}\\ \varepsilon^{(1)}_{\theta(s)}\\ \gamma^{(1)}_{x\theta(s)}\end{bmatrix}\quad(2)$$

其中,

$$\begin{bmatrix}\varepsilon^{(0)}_{x(s)}\\ \varepsilon^{(0)}_{\theta(s)}\\ \gamma^{(0)}_{x\theta(s)}\end{bmatrix}=\begin{bmatrix}\dfrac{\partial u_{0(s)}}{\partial x_{(s)}}+\dfrac{1}{2}\left(\dfrac{\partial w_{0(s)}}{\partial x_{(s)}}\right)^2\\ \left\{\dfrac{1}{R_{(s)}\cos\psi}\dfrac{\partial v_{0(s)}}{\partial\theta_{(s)}}+\dfrac{1}{R_{(s)}}w_{0(s)}+\right.\\ \left.\dfrac{1}{R_{(s)}}u_{0(s)}\tan\psi+\dfrac{1}{2}\dfrac{1}{R^2_{(s)}\cos^2\psi}\left(\dfrac{\partial w_{0(s)}}{\partial\theta_{(s)}}\right)^2\right\}\\ \left\{\dfrac{1}{R_{(s)}\cos\psi}\dfrac{\partial u_{0(s)}}{\partial\theta_{(s)}}-\dfrac{1}{R_{(s)}}v_{0(s)}\tan\psi+\right.\\ \left.\dfrac{\partial v_{0(s)}}{\partial x_{(s)}}+\dfrac{1}{R_{(s)}\cos\psi}\dfrac{\partial w_{0(s)}}{\partial x_{(s)}}\dfrac{\partial w_{0(s)}}{\partial\theta_{(s)}}\right\}\end{bmatrix}\quad(3)$$

$$\begin{bmatrix}\varepsilon^{(1)}_{x(s)}\\ \varepsilon^{(1)}_{\theta(s)}\\ \gamma^{(1)}_{x\theta(s)}\end{bmatrix}=\begin{bmatrix}\dfrac{\partial\varphi_{x(s)}}{\partial x_{(s)}}\\ \dfrac{1}{R_{(s)}\cos\psi}\dfrac{\partial\varphi_{\theta(s)}}{\partial\theta_{(s)}}+\dfrac{1}{R_{(s)}}\varphi_{x(s)}\tan\psi\\ \dfrac{1}{R_{(s)}\cos\psi}\dfrac{\partial\varphi_{x(s)}}{\partial\theta_{(s)}}-\dfrac{1}{R_{(s)}}\varphi_{\theta(s)}\tan\psi+\dfrac{\partial\varphi_{\theta(s)}}{\partial x_{(s)}}\end{bmatrix}\quad(4)$$

$$\begin{bmatrix}\gamma_{\theta z(s)}\\ \gamma_{xz(s)}\end{bmatrix}=\begin{bmatrix}\varphi_{\theta(s)}+\dfrac{1}{R_{(s)}\cos\psi}\dfrac{\partial w_{0(s)}}{\partial\theta_{(s)}}-\dfrac{1}{R_{(s)}}v_{0(s)}\\ \dfrac{\partial w_{0(s)}}{\partial x_{(s)}}+\varphi_{x(s)}\end{bmatrix}\quad(5)$$

壳的应力-应变关系可表示为

$$\begin{bmatrix}\sigma_{x(s)}\\ \sigma_{\theta(s)}\\ \sigma_{x\theta(s)}\\ \sigma_{\theta z(s)}\\ \sigma_{xz(s)}\end{bmatrix}=\begin{bmatrix}Q_{11}&Q_{12}&&&\\ Q_{12}&Q_{22}&&&\\ &&Q_{66}&&\\ &&&Q_{44}&\\ &&&&Q_{55}\end{bmatrix}\begin{bmatrix}\varepsilon_{x(s)}\\ \varepsilon_{\theta(s)}\\ \gamma_{x\theta(s)}\\ \gamma_{\theta z(s)}\\ \gamma_{xz(s)}\end{bmatrix}\quad(6)$$

其中,$Q_{mn}(m,n=1,2,4,5,6)$分别为

$$Q_{11}=Q_{22}=\frac{E(1-\nu)}{(1+\nu)(1-2\nu)}Q_{12}=\frac{E\nu}{(1+\nu)(1-2\nu)}$$

$$Q_{44}=Q_{55}=Q_{66}=\frac{E}{2(1+\nu)}\quad(7)$$

这里,E 表示杨氏模量,ν 表示泊松比.

根据 Hamilton 原理,得到系统的非线性动力学方程为:

$$a_{11}\frac{\partial^2 u_{0(s)}}{\partial x_{(s)}^2}+a_{12}\frac{\partial^2 u_{0(s)}}{\partial \theta_{(s)}^2}+a_{13}u_{0(s)}+a_{14}\frac{\partial v_{0(s)}}{\partial \theta_{(s)}}+$$
$$a_{15}\frac{\partial^2 v_{0(s)}}{\partial x_{(s)}\partial \theta_{(s)}}+a_{16}\left(\frac{\partial w_{0(s)}}{\partial \theta_{(s)}}\right)^2+a_{17}\frac{\partial w_{0(s)}}{\partial x_{(s)}}+$$
$$a_{18}\left(\frac{\partial w_{0(s)}}{\partial x_{(s)}}\right)^2+a_{19}\frac{\partial w_{0(s)}}{\partial x_{(s)}}\frac{\partial^2 w_{0(s)}}{\partial x_{(s)}^2}+$$
$$a_{20}\frac{\partial w_{0(s)}}{\partial x_{(s)}}\frac{\partial^2 w_{0(s)}}{\partial \theta_{(s)}^2}+a_{21}\frac{\partial w_{0(s)}}{\partial \theta_{(s)}}\frac{\partial^2 w_{0(s)}}{\partial x_{(s)}\partial \theta_{(s)}}+$$
$$a_{22}\frac{\partial^2 \varphi_{x(s)}}{\partial x_{(s)}^2}+a_{23}\frac{\partial^2 \varphi_{x(s)}}{\partial \theta_{(s)}^2}+a_{24}\frac{\partial \varphi_{\theta(s)}}{\partial \theta_{(s)}}+a_{25}\frac{\partial^2 \varphi_{\theta(s)}}{\partial x_{(s)}\partial \theta_{(s)}}$$
$$=a_{26}\ddot{u}_{0(s)}+a_{27}u_{0(s)}+a_{28}\dot{v}_{0(s)}+a_{29}v_{0(s)}+$$
$$a_{30}w_{0(s)}+a_{31x(s)}+a_{32}\varphi_{x(s)}+a_{33}\varphi_{\theta(s)}+$$
$$a_{34}\varphi_{\theta(s)}+a_{35} \tag{8a}$$

$$b_{11}\frac{\partial u_{0(s)}}{\partial \theta_{(s)}}+b_{12}\frac{\partial^2 u_{0(s)}}{\partial x_{(s)}\partial \theta_{(s)}}+b_{13}\frac{\partial^2 v_{0(s)}}{\partial x_{(s)}^2}+b_{14}\frac{\partial^2 v_{0(s)}}{\partial \theta_{(s)}^2}+$$
$$b_{15}v_{0(s)}+b_{16}\frac{\partial w_{0(s)}}{\partial \theta_{(s)}}+b_{17}\frac{\partial w_{0(s)}}{\partial x_{(s)}}\frac{\partial w_{0(s)}}{\partial \theta_{(s)}}+$$
$$b_{18}\frac{\partial w_{0(s)}}{\partial x_{(s)}}\frac{\partial^2 w_{0(s)}}{\partial x_{(s)}\partial \theta_{(s)}}+b_{19}\frac{\partial w_{0(s)}}{\partial \theta_{(s)}}\frac{\partial^2 w_{0(s)}}{\partial x_{(s)}^2}+$$
$$b_{20}\frac{\partial w_{0(s)}}{\partial \theta_{(s)}}\frac{\partial^2 w_{0(s)}}{\partial \theta_{(s)}^2}+b_{21}\frac{\partial \varphi_{x(s)}}{\partial \theta_{(s)}}+b_{22}\frac{\partial^2 \varphi_{x(s)}}{\partial x_{(s)}\partial \theta_{(s)}}+$$
$$b_{23}\frac{\partial^2 \varphi_{\theta(s)}}{\partial x_{(s)}^2}+b_{24}\frac{\partial^2 \varphi_{\theta(s)}}{\partial \theta_{(s)}^2}+b_{25}\varphi_{\theta(s)}$$
$$=b_{26}\ddot{u}_{0(s)}+b_{27}u_{0(s)}+b_{28}\ddot{v}_{0(s)}+b_{29}v_{0(s)}+$$
$$b_{30}w_{0(s)}+b_{31}\varphi_{x(s)}+b_{32}\ddot{\varphi}_{\theta(s)}+b_{33}\varphi_{x(s)}+$$
$$b_{34}\varphi_{\theta(s)}+b_{35} \tag{8b}$$

$$c_{11}\frac{\partial^2 u_{0(s)}}{\partial x_{(s)}^2}\frac{\partial w_{0(s)}}{\partial x_{(s)}}+c_{12}\frac{\partial^2 u_{0(s)}}{\partial \theta_{(s)}^2}\frac{\partial w_{0(s)}}{\partial x_{(s)}}+$$
$$c_{13}\frac{\partial^2 u_{0(s)}}{\partial x_{(s)}\partial \theta_{(s)}}\frac{\partial w_{0(s)}}{\partial \theta_{(s)}}+c_{14}\frac{\partial u_{0(s)}}{\partial x_{(s)}}+$$
$$c_{15}\frac{\partial u_{0(s)}}{\partial x_{(s)}}\frac{\partial w_{0(s)}}{\partial x_{(s)}}+c_{16}\frac{\partial u_{0(s)}}{\partial \theta_{(s)}}\frac{\partial w_{0(s)}}{\partial \theta_{(s)}}+c_{17}u_{0(s)}+$$
$$c_{18}u_{0(s)}\frac{\partial w_{0(s)}}{\partial x_{(s)}}+c_{19}\frac{\partial^2 v_{0(s)}}{\partial x_{(s)}^2}\frac{\partial w_{0(s)}}{\partial \theta_{(s)}}+$$
$$c_{20}\frac{\partial^2 v_{0(s)}}{\partial \theta_{(s)}^2}\frac{\partial w_{0(s)}}{\partial \theta_{(s)}}+c_{21}\frac{\partial^2 v_{0(s)}}{\partial x_{(s)}\partial \theta_{(s)}}\frac{\partial w_{0(s)}}{\partial x_{(s)}}+$$
$$+c_{22}\frac{\partial v_{0(s)}}{\partial \theta_{(s)}}+c_{23}\frac{\partial v_{0(s)}}{\partial \theta_{(s)}}\frac{\partial w_{0(s)}}{\partial x_{(s)}}+c_{24}v_{0(s)}\frac{\partial w_{0(s)}}{\partial \theta_{(s)}}+$$
$$c_{25}\frac{\partial^2 w_{0(s)}}{\partial x_{(s)}^2}+c_{26}\frac{\partial^2 w_{0(s)}}{\partial x_{(s)}^2}\left(\frac{\partial w_{0(s)}}{\partial x_{(s)}}\right)^2+$$
$$c_{27}\frac{\partial^2 w_{0(s)}}{\partial \theta_{(s)}^2}\left(\frac{\partial w_{0(s)}}{\partial x_{(s)}}\right)^2+c_{28}\frac{\partial^2 w_{0(s)}}{\partial \theta_{(s)}^2}\frac{\partial w_{0(s)}}{\partial \theta_{(s)}}+$$
$$c_{29}\frac{\partial^2 w_{0(s)}}{\partial \theta_{(s)}^2}\left(\frac{\partial w_{0(s)}}{\partial x_{(s)}}\right)^2+c_{30}\frac{\partial^2 w_{0(s)}}{\partial \theta_{(s)}^2}\left(\frac{\partial w_{0(s)}}{\partial \theta_{(s)}}\right)^2+$$
$$c_{31}\frac{\partial w_{0(s)}}{\partial x_{(s)}}\frac{\partial w_{0(s)}}{\partial \theta_{(s)}}\frac{\partial^2 w_{0(s)}}{\partial x_{(s)}\partial \theta_{(s)}}+c_{32}\frac{\partial w_{0(s)}}{\partial x_{(s)}}\left(\frac{\partial w_{0(s)}}{\partial \theta_{(s)}}\right)^2+$$
$$c_{33}\left(\frac{\partial w_{0(s)}}{\partial x_{(s)}}\right)^2+c_{34}\left(\frac{\partial w_{0(s)}}{\partial \theta_{(s)}}\right)^2+c_{35}w_{0(s)}\frac{\partial w_{0(s)}}{\partial x_{(s)}}+$$
$$c_{36}w_{0(s)}+c_{37}\frac{\partial^2 \varphi_{x(s)}}{\partial x_{(s)}^2}\frac{\partial w_{0(s)}}{\partial x_{(s)}}+c_{38}\frac{\partial^2 \varphi_{x(s)}}{\partial \theta_{(s)}^2}\frac{\partial w_{0(s)}}{\partial x_{(s)}}+$$
$$c_{39}\frac{\partial^2 \varphi_{x(s)}}{\partial x_{(s)}\partial \theta_{(s)}}\frac{\partial w_{0(s)}}{\partial \theta_{(s)}}+c_{40}\frac{\partial \varphi_{x(s)}}{\partial x_{(s)}}+c_{41}\frac{\partial \varphi_{x(s)}}{\partial x_{(s)}}\frac{\partial w_{0(s)}}{\partial x_{(s)}}+$$
$$c_{42}\frac{\partial \varphi_{x(s)}}{\partial \theta_{(s)}}\frac{\partial w_{0(s)}}{\partial \theta_{(s)}}+c_{43}\varphi_{x(s)}\frac{\partial w_{0(s)}}{\partial x_{(s)}}+c_{44}\varphi_{x(s)}+$$
$$c_{45}\frac{\partial^2 \varphi_{\theta(s)}}{\partial x_{(s)}^2}\frac{\partial w_{0(s)}}{\partial \theta_{(s)}}+c_{46}\frac{\partial^2 \varphi_{\theta(s)}}{\partial \theta_{(s)}^2}\frac{\partial w_{0(s)}}{\partial \theta_{(s)}}+$$
$$c_{47}\frac{\partial^2 \varphi_{\theta(s)}}{\partial x_{(s)}\partial \theta_{(s)}}\frac{\partial w_{0(s)}}{\partial x_{(s)}}+c_{48}\frac{\partial \varphi_{\theta(s)}}{\partial x_{(s)}}\frac{\partial w_{0(s)}}{\partial \theta_{(s)}}+$$
$$c_{49}\frac{\partial \varphi_{\theta(s)}}{\partial \theta_{(s)}}+c_{50}\frac{\partial \varphi_{\theta(s)}}{\partial \theta_{(s)}}\frac{\partial w_{0(s)}}{\partial x_{(s)}}+c_{51}\varphi_{\theta(s)}\frac{\partial w_{0(s)}}{\partial \theta_{(s)}}$$
$$=c_{52}i\ddot{w}_{0(s)}+c_{53}w_{0(s)}+c_{54}\dot{u}_{0(s)}+c_{55}u_{0(s)}+c_{56}v_{0(s)}+$$
$$c_{57}\ddot{\varphi}_{x(s)}+c_{58}\varphi_{x(s)}+c_{59}\varphi_{\theta(s)}+c_{60}+F_{(s)}-$$
$$\kappa\dot{w}_{0(s)}-(K_{(s)}+K_{(s-1)})w_{0(s)}(x_p,y_p)+$$
$$K_{(s)}w_{0(s+1)}(x_p,y_p)+K_{(s-1)}w_{0(s-1)}(x_p,y_p) \tag{8c}$$

$$d_{11}\frac{\partial^2 u_{0(s)}}{\partial x_{(s)}^2}+d_{12}\frac{\partial^2 u_{0(s)}}{\partial \theta_{(s)}^2}+d_{13}u_{0(s)}+d_{14}\frac{\partial v_{0(s)}}{\partial \theta_{(s)}}+$$
$$d_{15}\frac{\partial^2 v_{0(s)}}{\partial x_{(s)}\partial \theta_{(s)}}+d_{16}\frac{\partial w_{0(s)}}{\partial x_{(s)}}+d_{17}w_{0(s)}+$$
$$d_{18}\frac{\partial w_{0(s)}}{\partial x_{(s)}}\frac{\partial^2 w_{0(s)}}{\partial x_{(s)}^2}+d_{19}\frac{\partial w_{0(s)}}{\partial x_{(s)}}\frac{\partial^2 w_{0(s)}}{\partial \theta_{(s)}^2}+$$
$$d_{20}\frac{\partial w_{0(s)}}{\partial \theta_{(s)}}\frac{\partial^2 w_{0(s)}}{\partial x_{(s)}\partial \theta_{(s)}}+d_{21}\frac{\partial^2 \varphi_{x(s)}}{\partial x_{(s)}^2}+d_{22}\frac{\partial^2 \varphi_{x(s)}}{\partial \theta_{(s)}^2}+$$
$$d_{23}\varphi_{x(s)}+d_{24}\frac{\partial \varphi_{\theta(s)}}{\partial \theta_{(s)}}+d_{25}\frac{\partial^2 \varphi_{\theta(s)}}{\partial x_{(s)}\partial \theta_{(s)}}$$
$$=d_{26}\ddot{u}_{0(s)}+d_{27}u_{0(s)}+d_{28}\dot{v}_{0(s)}+d_{29}v_{0(s)}+$$
$$d_{30}w_{0(s)}+d_{31}\ddot{\varphi}_{x(s)}+d_{32}\varphi_{x(s)}+d_{33}\ddot{\varphi}_{\theta(s)}+$$
$$d_{34}\varphi_{\theta(s)}+d_{35} \tag{8d}$$

$$e_{11}\frac{\partial u_{0(s)}}{\partial \theta_{(s)}}+e_{12}\frac{\partial^2 u_{0(s)}}{\partial x_{(s)}\partial \theta_{(s)}}+e_{13}\frac{\partial^2 v_{0(s)}}{\partial x_{(s)}^2}+e_{14}\frac{\partial^2 v_{0(s)}}{\partial \theta_{(s)}^2}+$$
$$e_{15}v_{0(s)}+e_{16}\frac{\partial w_{0(s)}}{\partial \theta_{(s)}}+e_{17}\frac{\partial w_{0(s)}}{\partial x_{(s)}}\frac{\partial w_{0(s)}}{\partial \theta_{(s)}}+$$

$$e_{18}\frac{\partial w_{0(s)}}{\partial x_{(s)}}\frac{\partial^2 w_{0(s)}}{\partial x_{(s)}\partial\theta_{(s)}}+e_{19}\frac{\partial w_{0(s)}}{\partial\theta_{(s)}}\frac{\partial^2 w_{0(s)}}{\partial x_{(s)}^2}+$$
$$e_{20}\frac{\partial w_{0(s)}}{\partial\theta_{(s)}}\frac{\partial^2 w_{0(s)}}{\partial\theta_{(s)}^2}+e_{21}\frac{\partial\varphi_{x(s)}}{\partial\theta_{(s)}}+e_{22}\frac{\partial^2\varphi_{x(s)}}{\partial x_{(s)}\partial\theta_{(s)}}+$$
$$e_{23}\frac{\partial^2\varphi_{\theta(s)}}{\partial x_{(s)}^2}+e_{24}\frac{\partial^2\varphi_{\theta(s)}}{\partial\theta_{(s)}^2}+e_{25}\varphi_{\theta(s)}$$
$$=e_{26}\dot{u}_{0(s)}+e_{27}u_{0(s)}+e_{28}\ddot{v}_{0(s)}+e_{29}v_{0(s)}+$$
$$e_{30}w_{0(s)}+e_{31}\varphi_{x(s)}+e_{32}\varphi_{x(s)}+e_{33}\ddot{\varphi}_{\theta(s)}+$$
$$e_{34}\varphi_{\theta(s)}+e_{35}-M_{(s)}+\gamma\dot{\varphi}_{\theta(s)} \tag{8e}$$

其中,$R_{(s)}=r_{root}-x_{(s)}\tan\psi_{(s)}$,且$(s=1,2)$,边界条件为:

$$x_{(s)}=0,$$
$$u_{0(s)}=v_{0(s)}=w_{0(s)}=\varphi_{x(s)}=\varphi_{\theta(s)}=0 \tag{9a}$$
$$x_{(s)}=L,$$
$$N_{xx(s)}=N_{\theta\theta(s)}=N_{x\theta(s)}=M_{xx(s)}=M_{\theta\theta(s)}=M_{x\theta(s)}$$
$$=Q_{x(s)}=Q_{\theta(s)}=0 \tag{9b}$$
$$\theta_{(s)}=-\frac{\pi}{2}\text{和}\frac{\pi}{2},$$
$$N_{xx(s)}=N_{\theta\theta(s)}=N_{x\theta(s)}=M_{xx(s)}=M_{\theta\theta(s)}=M_{x\theta(s)}$$
$$=Q_{x(s)}=Q_{\theta(s)}=0 \tag{9c}$$

其中,$(s=1,2)$.

2　Galerkin 离散

对方程(8)进行无量纲化,然后应用 Galerkin 方法将偏微分形式的非线性方程离散为常微分形式的非线性动力学方程. 本文主要研究外界激励对系统振动的影响,选取了系统前两阶振动模态进行二阶 Galerkin 离散,在满足位移边界条件的情况下选取振型函数为[11]:

$$u_{0(s)}(x_{(s)},\theta_{(s)},t)$$
$$=u_{1(s)}(t)\cos(\frac{\pi}{L_{(s)}}x_{(s)})\cos(3\theta_{(s)}-3x_{(s)})+$$
$$u_{2(s)}(t)\cos(\frac{3\pi}{L_{(s)}}x_{(s)})\cos(\theta_{(s)}-x_{(s)}) \tag{10a}$$

$$v_{0(s)}(x_{(s)},\theta_{(s)},t)$$
$$=v_{1(s)}(t)\sin(\frac{\pi}{L_{(s)}}x_{(s)})\sin(3\theta_{(s)}-3x_{(s)})+$$
$$v_{2(s)}(t)\sin(\frac{3\pi}{L_{(s)}}x_{(s)})\sin(\theta_{(s)}-x_{(s)}) \tag{10b}$$

$$w_{0(s)}(x_{(s)},\theta_{(s)},t)$$
$$=w_{1(s)}(t)\sin(\frac{\pi}{L_{(s)}}x_{(s)})\cos(3\theta_{(s)}-3x_{(s)})+$$
$$w_{2(s)}(t)\sin(\frac{3\pi}{L_{(s)}}x_{(s)})\cos(\theta_{(s)}-x_{(s)}) \tag{10c}$$

$$\varphi_{x(s)}(x_{(s)},\theta_{(s)},t)$$
$$=\varphi_{x1(s)}(t)\cos(\frac{\pi}{L_{(s)}}x_{(s)})\cos(3\theta_{(s)}-3x_{(s)})+$$
$$\varphi_{x2(s)}(t)\cos(\frac{3\pi}{L_{(s)}}x_{(s)})\cos(\theta_{(s)}-x_{(s)}) \tag{10d}$$

$$\varphi_{\theta(s)}(x_{(s)},\theta_{(s)},t)$$
$$=\varphi_{\theta1(s)}(t)\sin(\frac{\pi}{L_{(s)}}x_{(s)})\sin(3\theta_{(s)}-3x_{(s)})+$$
$$\varphi_{\theta2(s)}(t)\sin(\frac{3\pi}{L_{(s)}}x_{(s)})\sin(\theta_{(s)}-x_{(s)}) \tag{10e}$$

其中,$(s=1,2)$.

利用 Galerkin 法进行离散,得到常微分方程:

$$\ddot{w}_{1(s)}+\mu_{1(s)}\dot{w}_{1(s)}+\omega_{1(s)}^2w_{1(s)}+$$
$$\alpha_{1(s)}\Omega_v\cos\omega_rtw_{1(s)}+\alpha_{2(s)}\Omega_v{}^2(\cos\omega_rt)^2w_{1(s)}+$$
$$\alpha_{3(s)}w_{1(s)}^2+\alpha_{4(s)}w_{2(s)}^2+\alpha_{5(s)}w_{1(s)}w_{2(s)}+$$
$$\alpha_{6(s)}w_{1(s)}^2w_{2(s)}+\alpha_{7(s)}w_{1(s)}^3+\alpha_{8(s)}w_{2(s)}^3+\alpha_{9(s)}+$$
$$\alpha_{10(s)}\Omega_v\sin\omega_rt+\alpha_{11(s)}\Omega_v\cos\omega_rt+$$
$$\alpha_{12(s)}\Omega_v^2\cos^2\omega_rt+\alpha_{13(s)}w_{1(s)}+\alpha_{14(s)}w_{1(s+1)}+$$
$$\alpha_{15(s)}w_{1(s-1)}=\alpha_{16(s)}F_{1(s)}\cos\omega_rt \tag{11a}$$

$$\ddot{w}_{2(s)}+\mu_{2(s)}\dot{w}_{2(s)}+\omega_{2(s)}^2w_{2(s)}+$$
$$\beta_{1(s)}\Omega_v\cos\omega_rtw_{2(s)}+\beta_{2(s)}\Omega_v{}^2(\cos\omega_rt)^2w_{2(s)}+$$
$$\beta_{3(s)}w_{1(s)}^2+\beta_{4(s)}w_{2(s)}^2+\beta_{5(s)}w_{1(s)}w_{2(s)}+$$
$$\beta_{6(s)}w_{1(s)}^2w_{2(s)}+\beta_{7(s)}w_{1(s)}^3+\beta_{8(s)}w_{2(s)}^3+$$
$$\beta_{9(s)}+\beta_{10(s)}\Omega_v\sin\omega_rt+\beta_{11(s)}\Omega_v\cos\omega_rt+$$
$$\beta_{12(s)}\Omega_v^2\cos^2\omega_rt+\beta_{13(s)}w_{2(s)}+\beta_{14(s)}w_{2(s+1)}+$$
$$\beta_{15(s)}w_{2(s-1)}=\beta_{16(s)}F_{1(s)}\cos\omega_rt \tag{11b}$$

其中$(s=1,2)$.

3　算例分析

考虑具有如下几何参数和材料属性的旋转圆锥壳 $L_{(s)}=0.15\text{m}$, $r_{\text{root}(s)}=0.1\text{m}$, $\psi_{(s)}=\frac{\pi}{6}$, $\nu=0.33$, $E=102.04\text{GPa}$, $h_{0(s)}=0.01\text{m}$, $\omega_r=150$, $\alpha_{(s)}=\frac{\pi}{3}$, $\beta_{(s)}=\frac{\pi}{6}$, $\rho=4450\text{kg/m}^3$, $\kappa=300\text{Ns/m}$, $F_{0(s)}=1.5\times10^6\text{N/m}^2$, $\Omega_c=2500\text{r/min}$, $\gamma=300\text{Ns/m}$. 分析系统的周

期运动,通过 Runge-Kutta 法,得到时间历程图、相位图和功率谱密度.

3.1 扰动转速对叶片非线性动力学现象的影响

为了研究扰动转速对系统非线性动力学特性的影响,以 Ω_v 为控制参数,研究其对系统非线性动力学响应的影响.

选定参数 $\Omega_v=0.37$,画出 1 号叶片的波形图进行研究.图 2(a)(b)(c)(d)(e)分别是 1 号叶片的 $(t, w_{1(1)})$、$(t, w_{2(1)})$ 平面上的波形图,$(w_{1(1)},\dot{w}_{1(1)})$、$(w_{2(1)},\dot{w}_{2(1)})$ 平面上的相位图和功率谱密度.

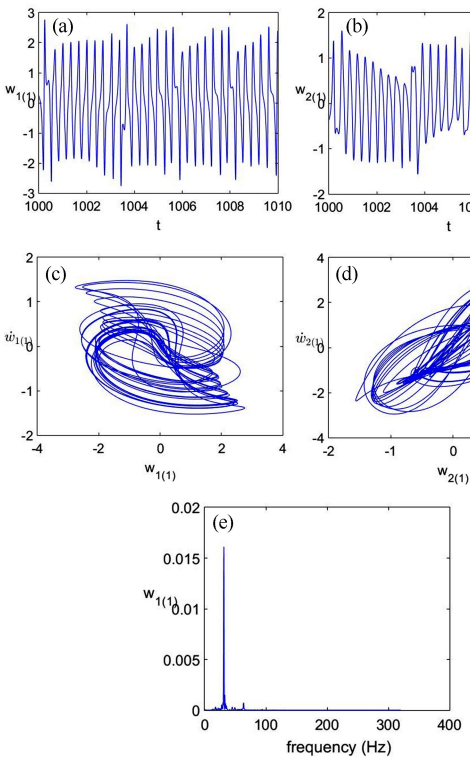

图 2 1 号叶片振动

Fig.2 Vibration of No.1 blade

选定参数 $\Omega_v=0.41$,画出 1 号叶片的波形图进行研究.图 3(a)(b)(c)(d)(e)分别是 1 号叶片的 $(t, w_{1(1)})$、$(t, w_{2(1)})$ 平面上的波形图,$(w_{1(1)},\dot{w}_{1(1)})$、$(w_{2(1)},\dot{w}_{2(1)})$ 平面上的相位图和功率谱密度.

通过分析,可以看出扰动速度对圆锥壳的影响.首先可以观察到悬臂圆锥壳存在稳态振动.其次,当圆锥壳的转速增加的时候,如图 2 和图 3 可以看到,伴随旋转速度的增加,w_1 和 w_2 的幅值有减小的趋势,该现象可解释为叶片在旋转过程中结构的刚度增加.

3.2 扰动力对叶片非线性动力学现象的影响

为了研究扰动力对系统非线性动力学特性的影响,以 $F_{1(1)}$ 和 $F_{1(2)}$ 为控制参数,研究其对系统非线性动力学响应的影响.

选定参数 $F_{1(1)}=0.31$,画出系统的波形图进行研究.图 4(a)(b)(c)(d)(e)分别是 1 号叶片的 $(t,w_{1(1)})$、$(t,w_{2(1)})$ 平面上的波形图,$(w_{1(1)},\dot{w}_{1(1)})$、$(w_{2(1)},\dot{w}_{2(1)})$ 平面上的相位图和功率谱密度.

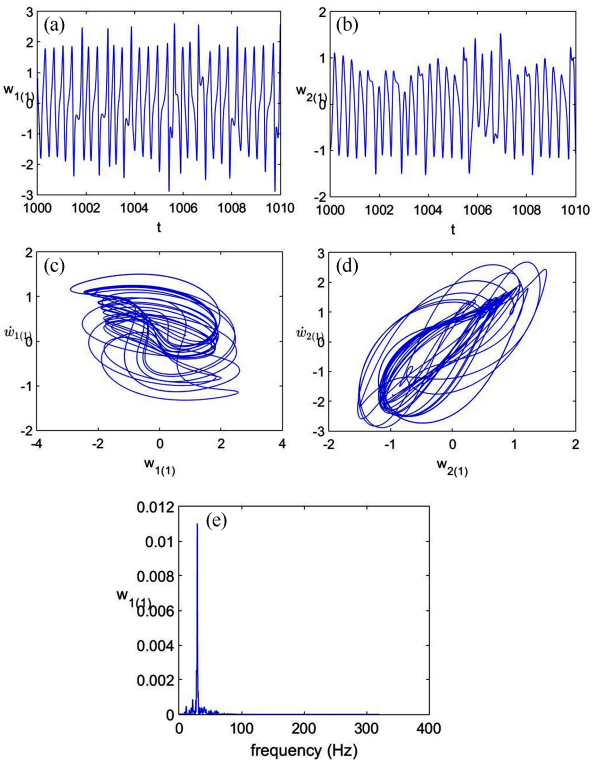

图 3 1 号叶片振动

Fig.3 Vibration of No.1 blade

图 4(f)(g)(h)(i)(j)分别是 2 号叶片的 $(t,w_{1(2)})$、$(t,w_{2(2)})$ 平面上的波形图,$(w_{1(2)},\dot{w}_{1(2)})$、$(w_{2(2)},\dot{w}_{2(2)})$ 平面上的相位图和功率谱密度.

选定参数 $F_{1(2)}=0.8$,画出系统的波形图进行研究.图 5(a)(b)(c)(d)(e)分别是 1 号叶片的 $(t,w_{1(1)})$、$(t,w_{2(1)})$ 平面上的波形图,$(w_{1(1)},\dot{w}_{1(1)})$、$(w_{2(1)},\dot{w}_{2(1)})$ 平面上的相位图和功率谱密度.

图 5(f)(g)(h)(i)(j)分别是 2 号叶片的 $(t,w_{1(2)})$、$(t,w_{2(2)})$ 平面上的波形图,$(w_{1(2)},\dot{w}_{1(2)})$、$(w_{2(2)},\dot{w}_{2(2)})$ 平面上的相位图和功率谱密度.

旋转悬臂圆锥壳上的横向外力增加后,w_1 和 w_2 的幅值增大;对于耦合振动系统,在不同叶片上加载不同的外力,对振动幅值有较大影响.

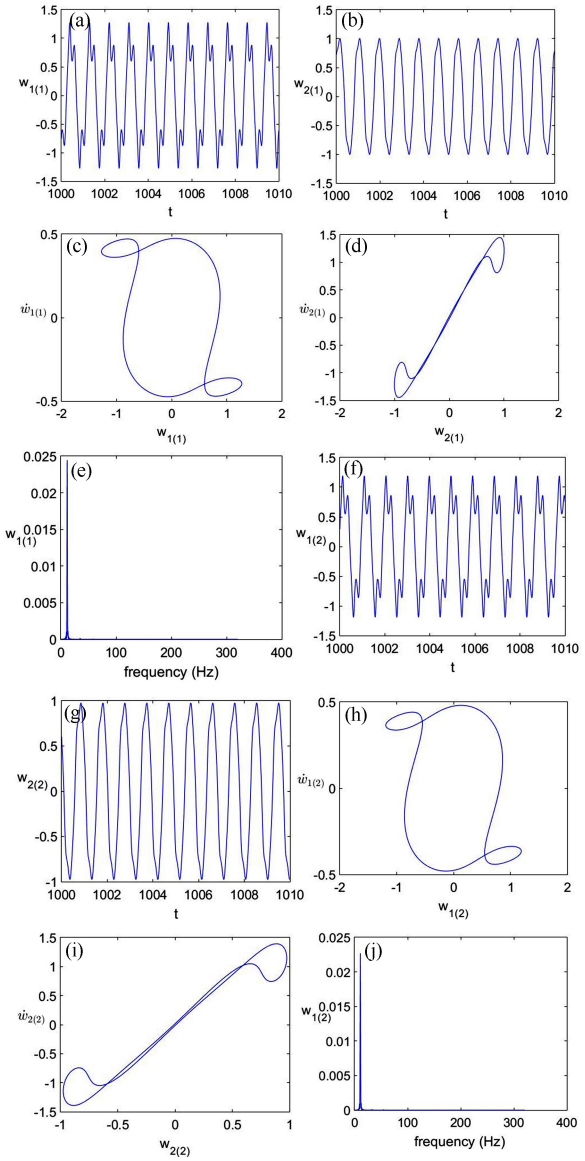

图 4　叶片振动

Fig.4　Vibration of the blades

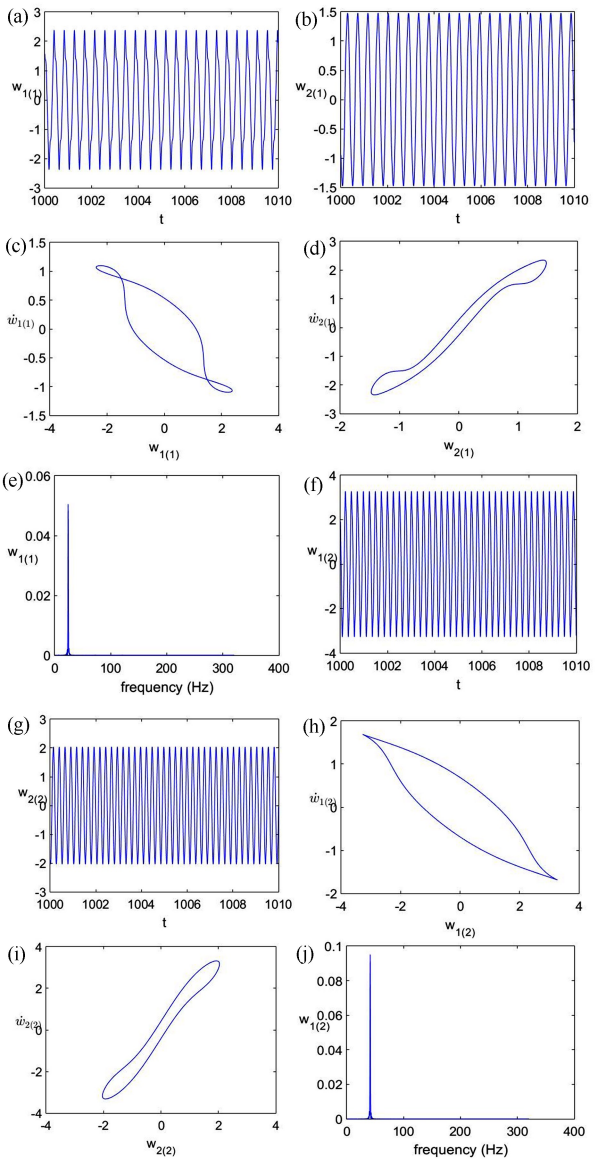

图 5　叶片振动

Fig.5　Vibration of the blades

4　结　论

本文提供了一个分析模型,用来研究变转速条件下双叶片整体叶盘的非线性动力学响应.从理论分析和数值结果可以得到下列结论:

(1)转速对整体叶盘叶片的振动幅值有影响,伴随旋转速度的增加,振动幅值减小,这个现象可解释为叶片在旋转过程中结构刚度增加;

(2)横向外力对整体叶盘叶片的振动有影响,伴随力的增大,振幅也增大;

(3)横向外力对整体叶盘的振动是一个重要的参数.对于耦合振动系统,在不同叶片上加载不同的外力,对振动幅值有较大影响.

参　考　文　献

1　Rao J S, Carnegie W. Solution of the equations of motion of coupled bending-bending-torsion vibrations of turbine blades by the method of Ritz-Galerkin. *International Journal of Mechanical Science*, 1970,12(10):875~882

2　Christensen E R, Lee S W. Nonlinear finite element modeling of the dynamics of unrestrained flexible structures. *Computers and Structures*, 1986,23(6):819~829

3　晏水平,黄树红,韩守木. 利用 Euler 梁模型计算汽轮机叶片静频和动频的传递矩阵法. 中国电机工程学报,2000,20(6):68~70 (Yan S P, Huang S H, Han S M. Tansfer matrix methods of static and dynamic frequencies calculation for turbine blades by using Euler beam model.

Proceedings of the CSEE, 2000,20(6):68~70 (in Chinese))

4 Yao M H, Chen Y P, Zhang W. Nonlinear vibrations of blade with varying rotating speed. *Nonlinear Dynamics*, 2012,68(4):487~504

5 Xiao S F, Chen B. Dynamic behavior of thin rectangular plate attached to moving rigid. *Applied Mathematics and Mechanics*, 2006,27(4):555~566

6 Hu X X, Tsuiji T. Free vibration analysis of rotation twisted cylindrical thin panels. *Journal of Sound and Vibration*, 1999,222(2):209~224

7 吴根勇,和兴锁,邓峰岩. 旋转复合材料板的动力学性能研究. 振动与冲击, 2008(8):149~154 (Wu G Y, He X S, Deng F Y. Dynamic analysis of a rotating composite plate. *Journal of Vibration and Shock*, 2008(8):149~154 (in Chinese))

8 Farhadi S, Hosseini-Hashemi S H. Aeroelastic behavior of cantilevered rotating rectangular plates. *International Journal of Mechanical Sciences*, 2011,53(4):316~328

9 邓军,陈国平. 匀速旋转弹性薄板分布动载荷时域识别. 振动、测试与诊断, 2011,31(6):724~727 (Deng J, Chen G P. Time-identification of distributed dynamic load for uniform rotating plate. *Journal of Vibration, Measurement & Diagnosis*, 2011,31(6):724~727 (in Chinese))

10 王晓峰,徐可君,秦海勤. 航空发动机风扇转子试验器动力学特性研究. 动力学与控制学报, 2017,15(2):142~148 (Wang X F, Xu K J, Qin H Q. Study on dynamic characteristics of aeroengine fan rotor tester. *Journal of Dynamics and Control*, 2017,15(2):142~148 (in Chinese))

11 Yang S W, Hao Y X, Zhang W, et al. Nonlinear dynamic behavior of functionally graded truncated conical shell under complex loads. *International Journal of Bifurcation and Chaos*, 2015,25(2):233

NONLINEAR VIBRATION ANALYSIS OF BLISK WITH TWO BLADES*

Jie Xiaobo† Zhang Wei

(*College of Mechanical Engineering, Beijing University of Technology, Beijing* 100124, *China*)

Abstract The nonlinear vibration responses of the blisk with two blades were investigated in this paper. The two rotating blades were settled as a springs-rotating conical shells system, and the effects of the presetting and pretwisted angles were considered for the model. Using Hamilton´s principle, the partial differential governing equation of the motion of blisk was established. Galerkin´s approach and numerical method were applied to analyze the nonlinear dynamics of the model. Numerical simulations were performed to investigate the responses of the blades under different rotating speeds and excitations. Numerical studies revealed the effects of the rotating speeds and excitations on the nonlinear vibration of the system.

Key words blisk, nonlinear dynamics, conical shell, Hamilton′s principle, Galerkin′s method

Received 13 March 2018, revised 21 May 2018.

* The project supported by the National Natural Science Foundation of China (11290152,11427801).

† Corresponding author E-mail: iron_man1945@163.com